Volume 10:1-13

The Undergraduate Journal of Experimental Microbiology & Immunology (+Peer Reviewed)

Harnessing the BrkA Autotransporter to Surface Display the Zinc-Binding Domain *Tetrahymena thermophila* Metallothionein MTT5 on *Escherichia coli* for Zinc Biosorption Evaluation

David Lin, Tiffany Lok Ting Wai, Alice Wang, Kevin Zhang

Department of Microbiology and Immunology, University of British Columbia, Vancouver, British Columbia, Canada

SUMMARY Heavy metal contamination, particularly zinc, poses significant environmental and health concerns. Surface expression of metal-binding proteins in easily culturable bacteria such as *Escherichia coli* presents a promising bioremediation strategy to mitigate heavy metal pollution. We investigated the surface expression of *Tetrahymena thermophila* metallothionein (MTT5), a 10.5 kDa metal-binding protein, using the BrkA autotransporter system in *E. coli*. We designed a recombinant BrkA-MTT5 plasmid (pADKT5) and confirmed MTT5 expression via western blot analysis. Further investigation utilizing a trypsin accessibility assay suggested the potential for BrkA-mediated export of MTT5. Additionally, the zinc-binding capacity of BrkA-MTT5 was evaluated by an *Arabidopsis thaliana* root growth assay which demonstrated statistically significant differences between bacteria-treated and non-treated conditions. Overall, these findings highlight the potential for BrkA-mediated export of MTT5 and lay the foundation for further research aimed at harnessing the bacterial surface display system for heavy metal bioremediation.

INTRODUCTION

Elevated heavy metal levels in ecosystems pose a health risk (1). Mining of common minerals can result in severe environmental contamination, leading to the release of heavy metals that pollute the air, water, and soil, and directly contribute to the emergence and aggravation of human diseases (2). This may also accumulate to toxic levels in plants, resulting in reduced growth (3). To address heavy metal contamination, bioremediation strategies are being explored as environmentally sensitive and cost-efficient alternatives to traditional methods that are both costly and labor-intensive (4, 5). A potential bioremediation strategy is to express recombinant metal-binding proteins on the surface of easily culturable bacteria such as *Escherichia coli* and incubate the culture in the contaminated environment for sequestration.

One study has shown the surface expression of putative cadmium-metallothionein (MTT5), a 10.5 kilodalton (kDa) protein from *Tetrahymena thermophila,* fused to the outer membrane lipoprotein and outer membrane protein A (Lpp-OmpA) complex in *E. coli* C43 (6, 7). The study showed an increase in cadmium (Cd) adsorption when incubated with *E. coli* C43 expressing MTT5, and a decrease in other Cd toxicity resistance genes, indicating additional protection conferred by the recombinant MTT5 (6). Espart *et al.* also demonstrated the ability of MTT5 to form stable complexes with Cd, Zn, and copper (8). Testing of Zn biosorption is a favorable alternative to Cd used in previous studies as excess Zn has been shown to negatively impact plant growth and productivity in the *Arabidopsis thaliana* model

Published Online: September 2024

Citation: Lin, Wai, Wang, Zhang. 2024. Harnessing the BrkA autotransporter to surface display the zinc-binding domain *Tetrahymena thermophila* metallothionein MTT5 on *Escherichia coli* for zinc biosorption evaluation. UJEMI+ 10:1-13

Editor: Ronja Kothe, University of British Columbia

Address correspondence to: https://jemi.microbiology.ubc.ca/

and offers a safer alternative than cadmium for research studies (6, 9). While Lpp-OmpA has been previously shown to mediate surface expression of functional MTT5, this system can potentially promote cell lysis and phenotype heterogeneity, hampering bioremediation efforts and highlighting the need for further investigation into other surface expression systems (10).

Serum resistance protein (BrkA) is a Type Va autotransporter secretion system found in *Bordetella pertussis*. Present in gram-negative bacteria, Type Va autotransporters are simple secretion systems where a single polypeptide sequence contains the secreted, modifiable passenger domain surrounded by the protein domains responsible for translocation across the inner and outer membranes (11). The Type Va secretion mechanism exploits an N-terminal signal sequence for transport across the inner membrane Sec translocase and a C-terminal translocation unit for movement across the outer membrane (12). Once secreted, the passenger domain can either remain anchored to the cell surface or be released to the extracellular space (11). Due to the simplicity and modularity of Type Va autotransporters, previous studies have shown the feasibility of exploiting this secretion pathway for expressing recombinant proteins (12, 13). A study by Sun et al. investigated the use of BrkA to express multiple proteins on the surface of *E. coli* using the BrkAutoDisplay vector (13). The study demonstrated the functional display of green fluorescent protein (GFP), catalytic enzymes, and single-chain antibodies (13). Importantly, BrkA was shown to display large (64 kDa) proteins, suggesting the possibility of translocating the 10.5 kDa MTT5 using the autotransporter for bioremediation purposes (13).

In this study, we hypothesize that the pENS plasmid, incorporating BrkA with a hexahistidine (6xHis) tag on a pDO6935 backbone, can facilitate the surface expression of functional MTT5 on *E. coli* UT5600 cells. To validate this hypothesis, we constructed a recombinant BrkA-MTT5 plasmid using the pENS backbone, confirmed MTT5 expression and export with western blot, and assessed MTT5 functionality through a novel *A. thaliana* growth assay. The successful expression and functional validation of MTT5 on the surface of *E. coli* cells indicate that this engineered system can be a powerful tool in bioremediation efforts. By enabling the display of MTT5, these engineered *E. coli* cells could be used to capture specific pollutants in contaminated environments for removal. Our preliminary findings set the foundation for developing microbial systems tailored for environmental cleanup, providing a more efficient and targeted approach to addressing pollution.

METHODS AND MATERIALS

Bacterial strains and growth conditions. Stocks of Top10 *E. coli* transformed with pADKT5, and UT5600 *E. coli* transformed with pADKT5 or pENS were grown overnight on Luria-Bertani (LB) plates with 1% agar and ampicillin (100 μg/mL) in 37°C incubator. For plasmid extraction, cells were grown in LB with ampicillin (100 μg/mL) broth overnight for 16 hours at 37°C, 200 rpm. UT5600 *E. coli* containing pADKT5, pDO6935, and pENS were grown in LB broth supplemented with ampicillin (100 μg/mL) with or without 5 mM beta-mercaptoethanol (βME) overnight at 37°C, 200 rpm and were harvested for protein extraction when optical densities at 600 nm (OD_{600}) reached 0.9 (Ultrospec 3000 Spectrophotometer). For the plant growth assay, 1 mL each of UT5600, containing pADKT5 and pENS, overnight cultures were used to inoculate two separate flasks of 49 mL LB broth supplemented with ampicillin (100 μg/mL) with or without 5 mM βME and grown overnight to OD_{600} of 0.6.

Gene block design. A gene block was designed using SnapGene™ and the sequence was sent to Integrated DNA Technologies (IDT) for construction. The MTT5 region was based on the 300 base pair (bp) coding region cDNA sequence from *T. thermophila* provided by Santovito et al. and contains a NsiI cut site (Fig 1B) (14). Additionally, TAA codons, which encode glutamine (Gln) instead of stop codons in *T. thermophila*, were changed to CAA which encodes Gln in *E. coli* to prevent the incorporation of a premature stop codon (7). A GGGGS linker sequence was added to both ends of the MTT5 gene to maintain the post-translational functionality and structure of the recombinant protein (15). Flanking the MTT5-GGGGS sequence was two 30 bp homologous regions upstream and downstream to the Thr^{481} and Pro^{482} amino acid junction of the pENS plasmid BrkA coding region (Fig 1A) (16). The full gene block amino acid sequence is depicted in Fig S2. The pENS plasmid, which contains a 6XHis tag near the N-terminus of BrkA, was generously provided by Goh et al. (16).

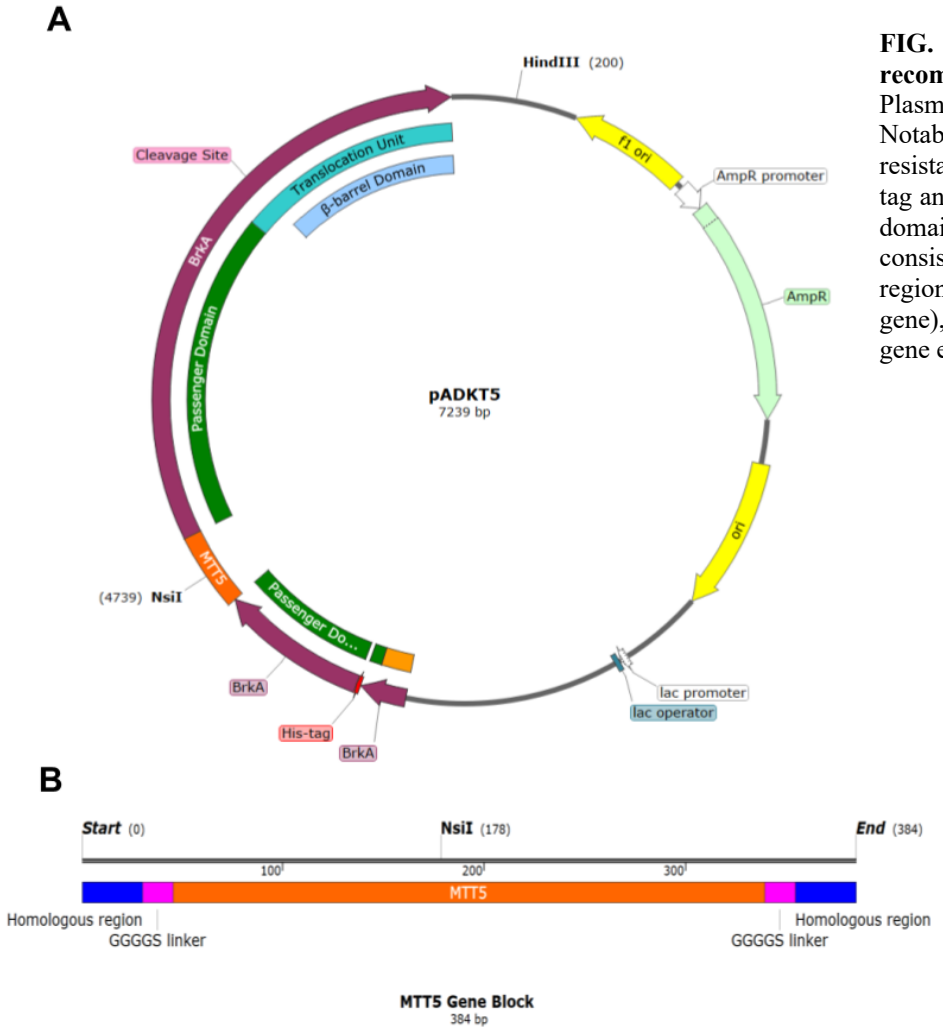

FIG. 1 Construction overview of the recombinant pADKT5 plasmid. A) Plasmid map of the 7,239 bp pADKT5. Notable features include an ampicillin resistance cassette, *brkA* gene with 6x His tag and MTT5 insertions in the passenger domain. B) MTT5 gene block design consisting of flanking homologous regions to the pENS backbone (*brkA* gene), flanking GGGGS linkers, and the gene encoding MTT5.

Primer design. Primers were designed to bind and linearize the pENS plasmid using SnapGene™ and sent to IDT for synthesis. MTT5_FWD (23 bp, 74% GC, T_m = 69.5°C) and MTT5_REV (22 bp, 70% GC, T_m = 66.7°C) were designed to bind upstream and downstream to the Thr^{481} and Pro^{482} junction in BrkA. Primer sequences are indicated in Figure S1.

PCR. 50 µL PCR reactions using the Q5® High-Fidelity DNA Polymerase (0.01U/µL, Biolabs) were prepared following the reaction mix recipe outlined in Table 1. 40 ng of template DNA was added for each sample and the equivalent volume of water was added as the negative control. PCR reactions were run in the Bio-Rad T100 Thermal Cycler with the conditions outlined in Table 2 for 25 cycles.

TABLE. 1 PCR reaction mix recipe for the linearization of pENS plasmid.

Component	Volume
5X Q5 reaction buffer	10 µL
Q5® High-Fidelity DNA Polymerase (0.01U/µL)	0.1 µL)
Template DNA or water	~1 µL (40 ng)
10 mM dNTP mix	1 µL
10 uM MTT5_FWD	2.5 µL
10 uM MTT5_REV	2.5 µL
DMSO	3.5 µL
Nuclease-free water	To 50 µL

TABLE. 2 Inverse PCR thermocycler settings for pENS plasmid.

Step	Temperature (°C)	Duration (seconds)
Initial denaturation	98	30
Denaturation	98	10
Annealing	72	150
Extension	72	120
Final extension	72	120

DpnI. 44 µL of PCR product was added to 5 µL of 10X rCutSmart Buffer and 1 µL of DpnI restriction enzyme. This solution was incubated for one hour at 37°C and then heat-inactivated at 80°C for 20 minutes.

DNA gel electrophoresis. Linearized pENS DNA samples were mixed in a 5:1 ratio with DNA Gel Loading Dye (6X) (ThermoFisher Scientific, Cat. #R0611) and ran on a 1% agarose gel following the Froggabio protocol. GeneRuler 1 kb DNA Ladder (ThermoFisher Scientific, Cat. #SM0311) was used, and gels were run for one hour at 120 volts (V). Gels were visualized on a BioRad GelDoc© system.

Linearized plasmid purification. Purification of PCR products and restriction digest products were performed using the QiaQuick PCR Purification Kit (Qiagen, Cat. #28104) as per manufacturer protocol. The purified PCR product was eluted in 50 µL of elution buffer.

Gibson assembly of ADKT5 gene block and pENS plasmid. Gibson assembly of the ADKT5 gene block and the linearized pENS plasmid vector was performed using the GeneArt™ Gibson Assembly EX Cloning Kit (Invitrogen, Cat. #A46633). The reaction consisted of a 2.8 µL vector, 0.95 µL of the ADKT5 gene block, 5 µL Master Mix A, and topped up to 10 µL with deionized water then incubated according to the manufacturer's recommended protocol. The reaction tube was placed on ice after incubation.

Transformation of TOP10 *E. coli* cells. Using the heat shock method, the Gibson assembly product was transformed into commercially competent TOP10 *E. coli* cells (Invitrogen, Cat. #A46633) according to the manufacturer's instructions. 100 µL of each transformation was spread on LB-Ampicillin (100 µg/mL) plates and then incubated at 37°C overnight.

Plasmid extraction from TOP10 transformants

TOP10 transformants grown on ampicillin-supplemented LB-agar plates were inoculated to liquid LB-ampicillin (100 µg/mL). Overnight cultures were subjected to plasmid extraction using the EZ-10 Spin Column Plasmid DNA Miniprep Kit (Bio Basic, Cat. #BS413) according to the manufacturer's instructions. Absorbance readings of the extracted DNA were collected using a microvolume spectrophotometer for concentration and purification assessments.

Restriction digest for product confirmation. pENS plasmids with the inserted gene block were subjected to restriction enzyme double digestion with NsiI (New England Biolabs, Cat. R0127S) and HindIII (New England Biolabs, Cat. #R0104S). The reaction mix recipe included 0.5 µg of plasmid DNA, 2.5 µL of 10X NEBuffer r2.1, 0.5 µL of NsiI, 0.5 µL of HindIII, and topped up with nuclease-free water for a total volume of 25 µL. The reaction mix was incubated at 37°C for one hour before heat inactivation at 80°C for 20 minutes. Digested plasmids were run with 6X loading dye on a 1% agarose gel with RedSafe Nucleic Acid Staining Solution (FroggaBio, Cat. #21141) at 100V for 60 min, and visualized on a transilluminator.

pADKT5 Sequencing. Overnight cultures of TOP10 *E. coli* cells containing pADKT were isolated and purified using the EZ-10 Spin Column Plasmid DNA Miniprep Kit, following the manufacturer's protocol. Three colonies with purified plasmid were diluted to 30 ng/µL. Dilutions (20 µL) were sent to Plasmidsaurus for nanopore sequencing. One purified plasmid was chosen to proceed as it was the correct sequence. One plasmid had random nucleotide

insertions and another had an additional adenosine added to the end of the gene encoding BrkA.

Preparing chemically competent UT5600 *E. coli* cells. *E. coli* UT5600 colony was inoculated in 2 mL of LB at 37°C for 200 rpm overnight. 1 mL of overnight culture was added to 99 mL of fresh LB and incubated on the shaker at 37°C for 200 rpm until OD 0.4. The culture was separated into two ice-cold Oakridge tubes and placed on ice for 20 minutes, then centrifuged at 4°C at 4000 rpm for 10 minutes. The supernatant was removed and the pellet was resuspended with 20 mL ice-cold 0.1M $CaCl_2$ and the suspension was incubated on ice for 30 minutes. The supernatant was discarded after centrifuging the suspension at 4°C at 4,000 rpm for 10 minutes. The pellet was resuspended in 5 mL ice-cold 0.1M $CaCl_2$ with 10% glycerol, incubated on ice for one hour, and then separated into 200 µL aliquots. Competent cells were stored at -80°C.

Transformation of UT5600 *E. coli* cells. 200 µL aliquots of competent cells were thawed on ice. 1 µL of pADKT5, pENS, and pDO6935 plasmid (100 ng/µL) were added to the aliquots and mixed by flicking. Mixtures were incubated on ice for 30 minutes. Mixtures were then transferred to a 42°C water bath for 30 seconds and immediately incubated on ice for two minutes. 1 mL of SOC medium was added to mixtures and incubated at 37°C, 200 rpm for one hour. Serial dilutions of 100 µL were then spread on Amp (100 µg/mL) LB plates and incubated overnight at 37°C.

Protein Extraction. Two mL of cells from overnight cultures containing 5 mM βME (OD_{600} = 0.9) were harvested by centrifugation at 3,000 rpm for 10 minutes. The pellets were resuspended in 200 µL of phosphate-buffered saline (PBS) and centrifuged at 3,000 rpm for 10 minutes. Harvested cells were lysed in 100 µL of 2X Laemmli sample buffer (Bio-Rad, Cat# 1610737) containing 5% βME and incubated at 95°C for five minutes.

Trypsin Protein Extraction. 2 mL of cells from overnight cultures were centrifuged at 3,000 rpm for 10 minutes. The supernatant was removed, and the cell pellet was washed two times with 200 µL PBS. The cell pellet was resuspended in 200 µL of PBS. The suspension was divided into 100 µL for trypsin and non-trypsin conditions. For the trypsin condition, 2 µL of trypsin (10 mg/mL) was added to 100 µL of cell suspension. Trypsin condition was incubated at 37°C for 10 minutes. Cells were centrifuged at 3000 rpm for 10 minutes, after which the supernatant was removed and rinsed twice with 1X PBS. The pellet was resuspended with 100 µL 1X Laemmli sample buffer and 5% βME to deactivate the trypsin.

Western blotting. 12 µL of protein samples and 3 µL of PageRuler™ Plus Prestained Protein Ladder (ThermoFisher Scientific, Cat. #26619) were loaded to precast protein gels (Bio-Rad, #4568096). The protein gels were subjected to electrophoresis at 120V for 90 minutes and transferred to a polyvinylidene fluoride (PVDF) membrane overnight at 30V and 4°C. The membrane was blocked with 5% skim milk powder in 1% Tris-buffered saline with 0.1% Tween® 20 detergent (TBS-T) (20 mL) on an orbital shaker at 50 rpm for one hour. This was followed by incubation with anti-6XHis tag antibody (Invitrogen, Cat. #MA1-21315) (15 mL, 1:3000 dilution in 5% milk in TBS-T) for one hour at room temperature. The membrane was washed three times with 1X TBS-T for five minutes. The membrane was then incubated with HRP-conjugated goat anti-mouse IgG antibody (Invitrogen, Cat. #31430) (15 mL, 1:10000 dilution in 5% milk in TBS-T) for one hour at room temperature and washed three times with 1X TBS-T for five minutes. Chemiluminescence detection reagents from Clarity Max Western ECL Substrate (Bio-Rad, #1705062) were used 1:1 to detect protein bands with the ChemiDoc MP Imaging System (Bio-Rad). All steps following the membrane transfer were performed in the dark at room temperature.

Preparation of Murashige and Skoog zinc sulfate plates for plant growth assay. 4.4 g of Murashige and Skoog (MS) basal salt mixture (Millipore Sigma, Cat. #M5524) with 10 g of sucrose was added to one L of sterile dH_2O and autoclaved to make MS media with 1% sucrose. Five conditions of MS supplemented with varying concentrations of zinc sulfate

($ZnSO_4$) (0, 50, 100, 200, 300 μM) were made. Five 10 mL aliquots of each of the UT5600 overnight cultures were transferred into 10 separate sterile Oakridge tubes and centrifuged at 3,000 rpm for five minutes to pellet cells. Pellets were then washed twice with 1X PBS and centrifuged at 3,000 rpm for five minutes again. Each pellet was then resuspended in 20 mL of each MS with $ZnSO_4$ condition and transferred to a flask. Flasks were incubated in a 37°C shaking incubator for two hours. 20 mL of each MS with $ZnSO_4$ condition was also prepared without bacterial treatment. After incubation, MS media with $ZnSO_4$ treated with bacteria were aliquoted into Oakridge tubes and centrifuged at 3,000 rpm for five minutes. Supernatants were collected and 0.16 g of Phytogel (0.8% (w/v)) (Millipore Sigma, Cat. #P8169) was added to each tube and autoclaved. Each 20 mL aliquot was then used to pour individual plates.

Plant growth assay. *A. thaliana* ecotype Col-0 seeds were dry-stratified at 4°C in the dark for two days. Seeds were surface sterilized with 70% ethanol for five minutes, followed by 1% sodium hypochlorite (v/v) for 10 minutes. Sterilized seeds were then washed with four separate volumes of sterile dH_2O. 10 to 15 seeds were placed horizontally across each MS $ZnSO_4$ plate. Plates were sealed with micropore tape, placed vertically, and grown under continuous light conditions. Images of seedlings were taken with an iPhone 8+ camera at four, six, and nine days after germination (DAG). Primary root (PR) lengths were measured unblinded using ImageJ software. Only seeds that germinated at the same time were analyzed. Sample size per treatment varied between two to five seedlings due to germination rate.

Statistical Analysis. A two-way ordinary ANOVA with Tukey-Kramer's multiple comparison *post hoc* test was conducted to determine the observed effects of $ZnSO_4$ concentration and treatment condition on PR length on GraphPad Prism software. $P < 0.05$ was considered significant.

RESULTS

The pADKT5 recombinant plasmid was engineered by inserting the MTT5 protein into the BrkA autotransporter region of the pENS plasmid using Gibson assembly. Inverse PCR of the pENS plasmid was used to linearize the vector for Gibson assembly. The linearized vector, subjected to PCR purification and DpnI digestion, showed a distinct band at ~8000bp on a 1% agarose electrophoresis gel (Fig 2A). Gibson assembly was performed with the purified PCR product and the gene block. After transforming the Gibson assembly products to TOP10 competent *E. coli* cells, 12 colonies were subjected to plasmid extraction to screen for expression of pADKT5. Double restriction digestion with NsiI and HindIII of pADKT5 was expected to yield two distinct bands (2,016 bp, 5,253 bp) on an agarose electrophoresis gel. Two out of the three colonies (lanes eight, nine) showed two bands around 2,000 bp and 5,000 bp" (Fig 2B). As the NsiI cut site is unique to the MTT5 gene block, the appearance of the two bands demonstrated potential insertion by Gibson assembly. Nanopore sequencing confirmed the proper assembly of the recombinant plasmid from lane nine.

BrkA-MTT5 is expressed and exported to the cell surface in *E. coli*. To assess the expression of the BrkA-MTT5 protein, we performed an anti-6XHis tag western blot analysis using *E. coli* UT5600 cells (Fig 3). We anticipated observing two bands in the western blot: one at 114 kDa and one at 84 kDa. Western blot of the BrkA-MTT5 construct showed the presence of a singular band at ~130 kDa, likely corresponding to the intracellular, unprocessed protein (Fig 3A). Furthermore, the observed band at ~130 kDa d corresponds to the unprocessed, intracellular wildtype BrkA from pENS, indicating expression of BrkA-MTT5 (Fig 3A). Several low molecular weight bands were observed in all conditions, including the negative controls. These bands observed in western blots are likely not our protein of interest, which may be due to non-specific binding as our primary antibody only targets the 6X-His tag and there might be a protein with similar amino acid sequences, cross-reactivity, degradation products, contaminants, or be experimental artifacts. However, this initial blot did not demonstrate the presence of the expected, second 84 kDa processed, extracellular BrkA-MTT5 band.

A trypsin accessibility assay was conducted using overnight cultures supplemented with 5 mM βME to create reducing conditions (Fig 3B) to assess the surface expression of our

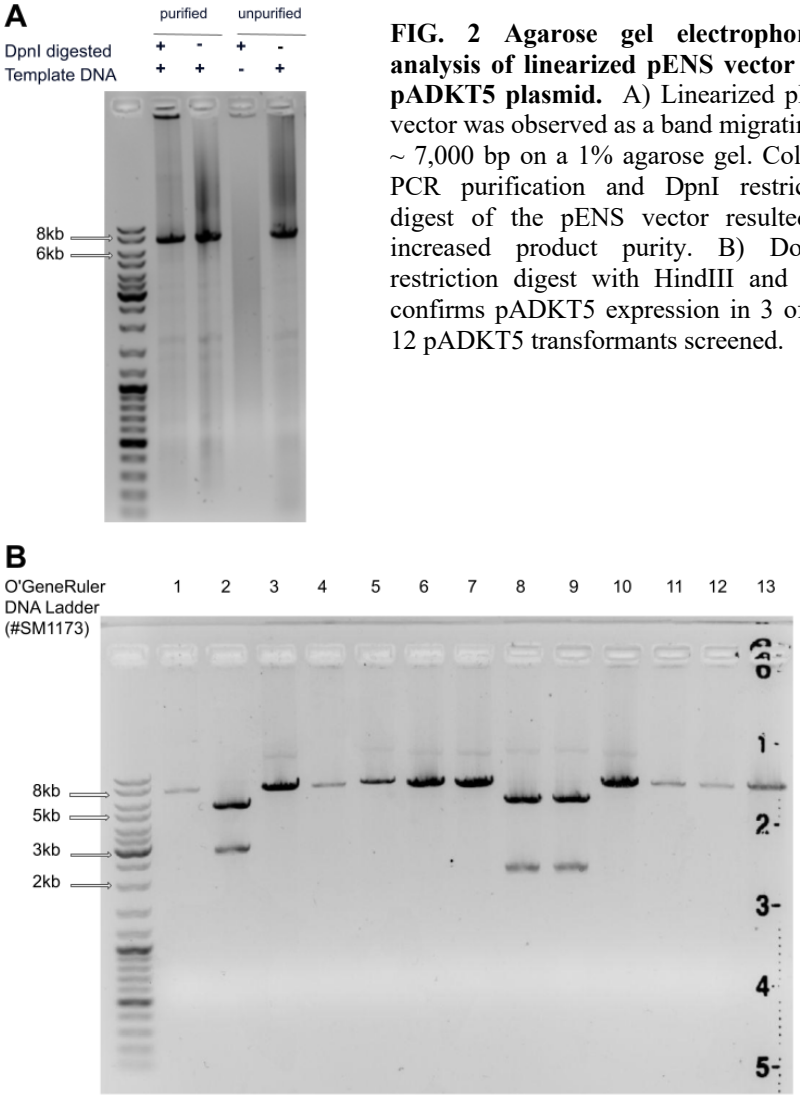

FIG. 2 Agarose gel electrophoresis analysis of linearized pENS vector and pADKT5 plasmid. A) Linearized pENS vector was observed as a band migrating at ~ 7,000 bp on a 1% agarose gel. Column PCR purification and DpnI restriction digest of the pENS vector resulted in increased product purity. B) Double restriction digest with HindIII and NsiI confirms pADKT5 expression in 3 of the 12 pADKT5 transformants screened.

BrkA-MTT5 construct. In pADKT lanes six, seven, and eight, the expected ~130 kDa intracellular BrkA-MTT5 was observed in the presence and absence of trypsin. Furthermore, there was an ~70 kDa band which corresponds to the processed, exported BrkA-MTT5 as shown by the disappearance of the band in the trypsin condition (Fig 3B). Interestingly, the observed ~70 kDa band in the pADKT5 7 lane was lower than the bands corresponding to the extracellular, processed BrkA from pENS which has an expected weight of73 kDa (17). However, this discrepancy is likely attributed to pENS rather than pADKT5, as the processed pENS band appeared to be heavier than expected (~100 kDa).

Bacterial treatment of MS with $ZnSO_4$ reduced *A. thaliana* seedling primary root length. To determine the functionality of our recombinant, surface-expressed BrkA-MTT5 construct in UT5600 *E. coli* cells, we designed a novel assay using *Arabidopsis thaliana* seedlings (Fig 4). Previous studies have shown that *A. thaliana* seedlings exposed to toxic levels of $ZnSO_4$ (> 100 µM) in MS media show reduced primary root length compared to 0 µM and 50 µM $ZnSO_4$ (9). For the assay, MS media treated with pENS controls for the effect of bacterial exposure on the seedling. If the BrkA-MTT5 construct is functional, *A. thaliana* seedlings grown in MS treated with pADKT5 will have greater primary root lengths compared to pENS-treated seedlings at $ZnSO_4$ concentrations above 100 µM. At 4 DAG, there was a significant interaction between the effects of the treatment condition and PR lengths (Fig 4A). At 6 DAG, significant differences were observed between the pADKT5 or pENS treated PR lengths compared with untreated (Fig 4B). At a $ZnSO_4$ concentration of 50

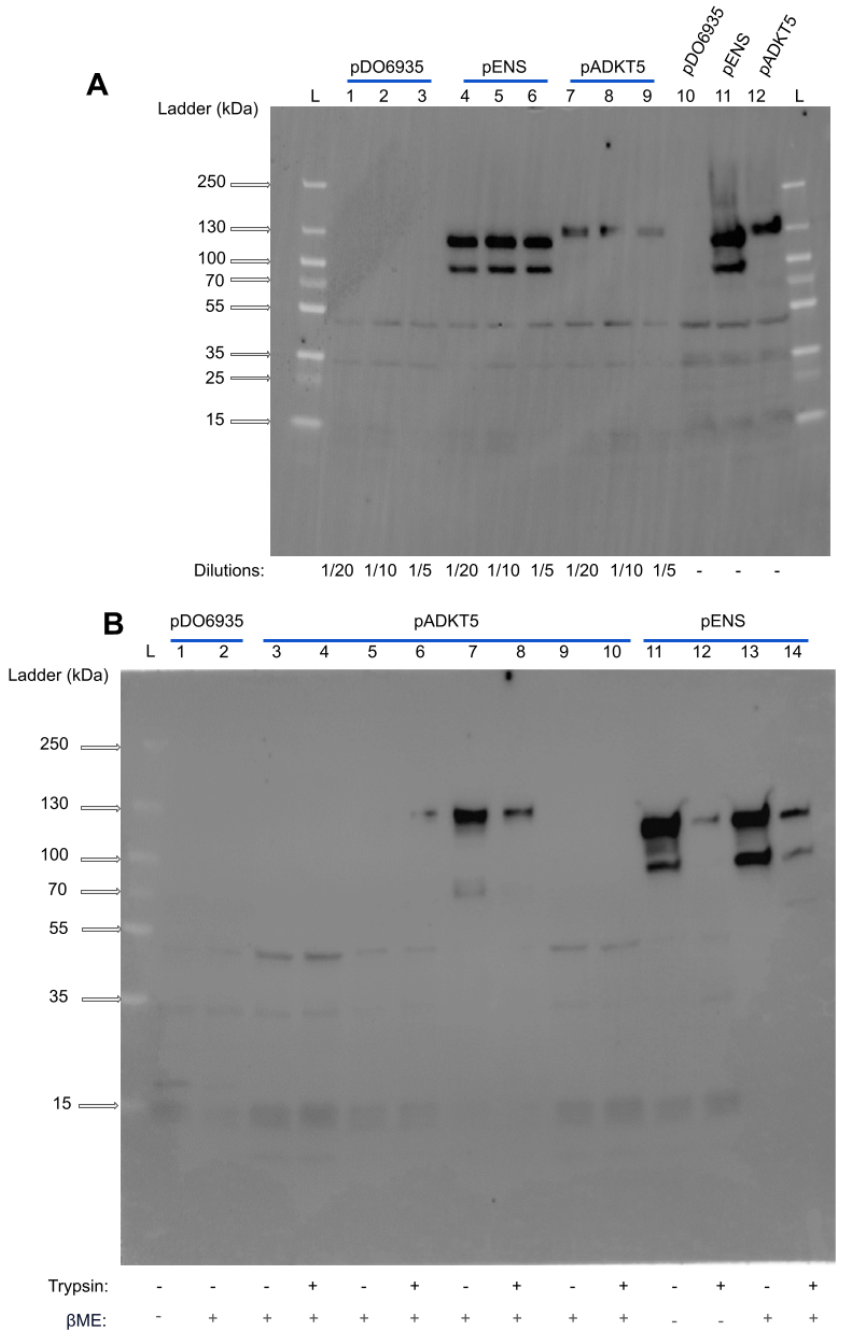

FIG. 3 BrkA-MTT5 is expressed and exported to the cell surface. (A) Western blot analysis of *E. coli* UT5600 protein lysates using anti-6XHis mouse antibody and detected with goat anti-mouse horseradish peroxidase. (B) Cells were treated with trypsin and /or BME (+) or without (-) as outlined in the methods. pDO6935 serves as the wild-type BrkA vector negative control, while pENS acts as the positive control. The PageRuler™ Plus Prestained Protein Ladder was used for size reference, with 130 kDa indicating the unprocessed intracellular BrkA-MTT5 binding domain and 84 kDa indicating the extracellular BrkA-MTT5 binding domain.

µM, untreated PR lengths were significantly different from pADKT5 treated (Fig 4B). Furthermore, at nine DAG, significant differences were observed between pADKT5 and pENS treatment and untreated PR lengths (Fig 4C). At 100 µM $ZnSO_4$, pADKT5 was significantly different from untreated (Fig 4C). For the 100 µM $ZnSO_4$ concentration at 6 DAG and the 50 µM $ZnSO_4$ at 9 DAG, no significant differences were observed between any of the plasmid conditions. Importantly, we did not observe a significant difference between pADKT5 and pENS treatments across all days and concentrations. However, this assay was conducted without the addition of βME to the overnight cultures, due to time constraints, which was shown previously to be potentially necessary for the surface expression of MTT5 (Fig 3). Despite the absence of βME, these results suggest that bacterial treatment, independent of the plasmid condition, of MS media supplemented with $ZnSO_4$ impairs *A. thaliana* seedling primary root length when compared to untreated control.

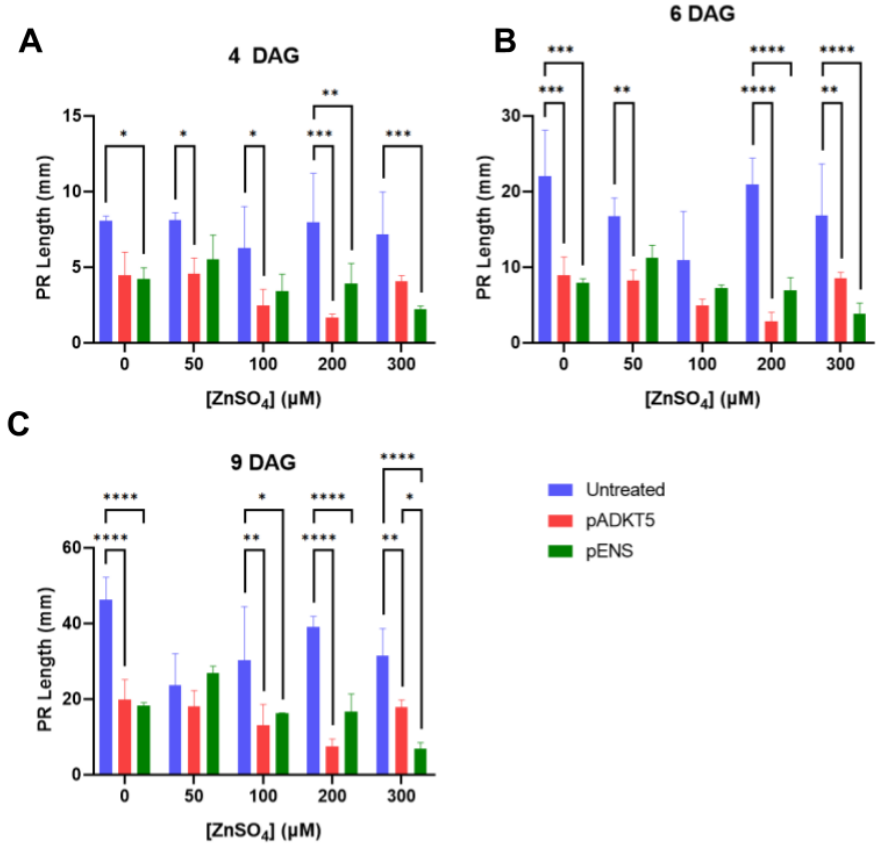

FIG. 4 Bacterial treatment of MS + $ZnSO_4$ reduced *A. thaliana* seedling primary root length. PR lengths observed in MS media supplemented with different $ZnSO_4$ concentrations (0, 50, 100, 200, 300 μM), treated with UT5600 *E. coli* cells carrying pADKT5 or pENS or left untreated. A) PR length at 4 DAG. B) PR length at 6 DAG. C) PR length at 9 DAG. Sample sizes between conditions were 2 - 5 seedlings. An ordinary two-way ANOVA with Tukey's multiple comparison *post hoc* test was conducted (* = P < 0.05, ** = P < 0.01, *** < 0.001, **** = P < 0.0001).

DISCUSSION

Our study aimed to investigate the ability of the recombinant BrkA-MTT5 protein to facilitate the export of MTT5 to the cell surface. Additionally, we evaluated the Zn-binding capacity of the BrkA-MTT5 protein by treating Zn-supplemented growth media with *E. coli* expressing BrkA-MTT5, then compared *A. thaliana* root growth in the different media. To achieve these aims, we constructed the recombinant plasmid through Gibson assembly and confirmed the presence of the MTT5 insert using Nanopore sequencing. Subsequently, we assessed the cell surface expression of MTT5 in *E. coli* via anti-6XHis western blot analysis and a trypsin accessibility assay.

The pADKT5 recombinant plasmid was constructed by the insertion of a custom gene block comprising the MTT5 domain into the BrkA passenger region/domain within the pENS plasmid. The AlphaFold structure of BrkA indicates that this region is unstructured and poorly characterized, suggesting that insertion of MTT5 here will likely not disrupt the folding of the passenger β-helix, and unimpeded translocation across the cell membrane would be maintained (18). The pENS plasmid was selected as the vector as it contains a 6X-His Tag insertion to BrkA. Plasmid linearization by inverse PCR was chosen for Gibson assembly vector construction due to the absence of a restriction enzyme cut site within the unstructured regions of the BrkA passenger domain (16). Forward and reverse primers amplifying in opposite directions from the insertion site were designed, with careful consideration of the primer lengths to optimize specificity and %GC content. The product of linearized plasmid on the agarose gel showed smearing (Fig 2A). This could be attributed to the non-specific binding of the primers and was resolved partially with the use of longer primers. Smearing could also be due to the overloading of genomic DNA as 40 ng of template was used. Additionally, our PCR thermocycler settings incorporated a final extension time identical to the cyclical extension time which could contribute to smearing due to incomplete extension. A distinct band was observed when the PCR products were purified and DpnI digested.

Double restriction digestion was performed with NsiI and HindIII as the NsiI cut site is unique to the MTT5 gene block. Therefore, the appearance of two bands at the expected molecular weight demonstrated the potential insertion of our gene block by Gibson assembly.

Only two of the 12 lanes showed two bands that were at the expected molecular weight for the double restriction digest. The inconsistent Gibson assembly results could be attributed to incomplete DpnI digestion of the non-linearized pENS template, leading to transformation with pENS without the MTT5 insert (19). Additionally, the failure to achieve a 1:1 ratio between the linearized plasmid and gene block could also have contributed to the observed outcome. An insufficient gene block-to-vector ratio could lead to the direct ligation of the linearized vector without the gene block insert. The normalization of gene block to vector was potentially inaccurate as it required quantifying linearized plasmid prepared from PCR which could have had leftover reagents that would have interfered with the spectrophotometer reading. While the A260/280 reading was within the expected range, it is possible that the PCR purification or DpnI digestion was not able to remove all the residual primers or circular plasmid which would inflate the yield without affecting the A260/280 reading. Additionally, due to our difficulty remedying the lane smearing, products from non-specific amplification could have inflated the DNA yield preventing an accurate 1:1 ratio from being achieved. As for lane two, although it showed two bands, the band size for the lower band was at ~3,000 bp instead of the expected size of ~2,000 bp. Plasmid nanopore sequencing results of the colonies corresponding to lanes two, eight, and nine indicated that only lane nine contained the correctly constructed pADKT5 plasmid. Sequencing results for lane two showed random nucleotide insertion mutations and the addition of a single non-templated adenosine to the end of the *brkA* gene for lane eight.

BrkA-MTT5 was expressed in the pADKT5 plasmid (Fig 3). In the pADKT5 samples, there was a band at ~130 kDa that corresponds to the expected size of intracellular BrkA-MTT5 (Fig 3A & B). Furthermore, this intracellular band appeared above the wildtype intracellular BrkA expressed from pENS, indicating that our constructed protein had higher molecular weight. However, this intracellular band was not present in all pADKT5 samples. Since BrkA is expressed constitutively at low levels, continuous production of the BrkA-MTT5 construct may be metabolically stressing for the cell (17, 20). This metabolic stress could potentially be toxic to the host bacteria, inhibiting growth and leading to host cell lysis and death (20). Furthermore, the addition of MTT5 could have increased metabolic demand compared with wild-type BrkA. Inhibition of growth or cell death decreases protein yield, which may explain the inconsistent pADKT5 signals observed. We also only observed the extracellular, processed ~70 kDa band in the pADKT5 condition after the addition of 5 mM βME to the culture (Fig 3B), suggesting reducing conditions in the culture are necessary for BrkA-MTT5 surface expression. Passenger domains rich in cysteine form disulfide bonds upon entry into the oxidizing conditions of the periplasm (21). Periplasmic disulfide bonds block type Va autotransporter translocation (21). Klauser et al. had previously shown that culturing *E. coli* UT5600 with 5 mM βME to create reducing conditions was necessary for the surface export of cysteine-rich cholera toxin B subunit using Iga_{β} (22). In addition to our expected bands, there were non-specific background bands observed in all conditions. Reducing the concentration of the protein lysate or antibodies may decrease non-specific binding (23).

The *A. thaliana* plant growth assay showed significant differences in primary root length between untreated and treated (pENS, pADKT5) conditions, but no differences in root length between pENS and pADKT5 conditions. Both treated conditions resulted in decreased primary root length growth. Microbial anabolism depends upon carbon and inorganic elements such as nitrogen, phosphorus, potassium, and magnesium for growth (24). These nutrients are also crucial for plant growth and were present in the MS media used in the experiment. It is plausible that during the incubation period with *E. coli* and MS Zn solutions, the bacteria absorbed a substantial amount of these nutrients, potentially leading to reduced availability for plant uptake and consequently minimizing plant growth. In addition, the *E. coli* may have altered the pH of the media, potentially shifting it to a pH range that is not conducive to optimal plant root growth which has been previously reported with other bacterial strains and plant species (25).

Limitations A limitation of this study lies in the choice of MTT5 as the protein for surface expression on *E. coli* cells. While MTT5 is capable of chelating Zn ions, there are more efficient metallothionein for this purpose (8). Previous research has demonstrated that other

metallothioneins, such as MTT3 and MTT1 from *T. thermophila,* exhibit superior Zn binding capabilities (8, 26). MTT3 contains two histidine residues, which have a higher affinity for Zn ions due to the imidazole rings of the histidines that stabilize metal-protein complexes (26). This suggests that the use of MTT3 or MTT1 could have potentially enhanced the effectiveness of our BrkA-metallothionein construct for bioremediation of Zn compared to our BrkA-MTT5 which showed no functionality in our *A. thaliana* assay.

Using genetically modified organisms (GMOs) for the bioremediation of Zn or other heavy metals presents several challenges that limit their effectiveness (27). One of the primary concerns is the ecological risk associated with introducing GMOs into natural environments, where they may disrupt indigenous soil microbiomes and struggle to compete with native microorganisms, leading to difficulties in establishing and maintaining their presence (27). Additionally, the stability of recombinant plasmids, which carry the biodegradation genes, is often compromised by environmental factors like pH, temperature, and salinity, reducing effectiveness (27). There is a significant risk of horizontal gene transfer between GMOs and native microbes, potentially leading to unintended ecological consequences, such as the spread of antibiotic resistance genes (27). Furthermore, various regulations and policies constrict the release of GMOs into the environment (27). To mitigate these risks, strategies like suicide genes and controlled release methods can be employed (27). Future research must carefully consider these limitations to develop more stable, effective, and environmentally safe bioremediation strategies that address the challenges posed by the use of GMOs in heavy metal remediation.

Conclusions Our investigation involved the construction of a BrkA-MTT5 (pADKT5) recombinant plasmid using Gibson assembly to elucidate the export of MTT5 protein via the BrkA autotransporter and to evaluate its capacity to bind Zn. Western blot analysis confirmed the presence of the expected intracellular BrkA-MTT5 band at ~114 kDa and the anticipated extracellular BrkA-MTT5 band at ~84 kDa when pADKT5 UT5600 *E. coli* cells were cultivated with βME. However, subsequent growth assays assessing *A. thaliana* growth yielded inconclusive outcomes due to the absence of βME in bacterial growth media, which would have not expressed the BrkA-MTT5 extracellularly. Nonetheless, the results obtained from the western blot and trypsin accessibility assay suggest the feasibility of BrkA autotransporter-mediated export of MTT5 protein, indicating promising steps for further investigations.

Future Directions The plant assay was conducted to assess the functionality of the expressed MTT5 protein, which was a key objective for our group. However, there were major limitations associated with this assay. For all conditions, only a small number of seeds germinated, leading to a small sample size. To achieve a more robust statistical analysis, a larger sample size is necessary such as a sample size of 50 used in a previous study by Wang et al. (9). Additionally, *E. coli* were not cultured in the presence of βME, and due to time restrictions, the assay was conducted before the results of our western blot with βME cultured cells. Thus, future studies could refine our preliminary *A. thaliana* assay to improve germination rates and increase sample size, while also including βME in the bacterial culture conditions.

Other methods to assess BrkA-MTT5 functionality can be investigated. Future studies could quantify the adsorption abilities by performing inductively coupled plasma mass spectrometry (ICP-MS). ICP-MS is an analytical technique that can quantitatively measure trace elements in biological samples, enabling the quantification of zinc binding by transformed bacteria. Given the capacity of MTT5 to bind other heavy metals, future studies can test its binding ability to other divalent metal cations such as cadmium and lead. Another bioassay involving *E. coli* transformed with pADKT5 and pENS cultured in LB media supplemented with a toxic concentration of Zn can be performed to determine biosorption. Assuming that the BrkA-MTT5 construct is functional and present on the cell surface, the *E. coli* containing pADKT5 would exhibit survival or growth, measured by OD600 readings, due to the detoxification of the media by the MTT5 protein.

The formation of disulfide bonds from the cysteine amino acid residues found in the MTT5 protein may inhibit efficient secretion by the BrkA autotransporter. This study

evaluated only one βME concentration (5 mM) as this concentration was shown to effectively induce surface expression of *Vibrio cholerae* toxin B in *E. coli* (22). It remains inconclusive whether this concentration is optimal for BrkA-MTT5 and incubation with other βME concentrations should be investigated. Another method of altering the oxidation environment of the protein would be to employ an *E. coli* strain that is disulfide bond (Dsb) formation negative. The use of this *E. coli* strain would lower the chance of disulfide bond formation when the BrkA-MTT5 folds in the periplasm.

ACKNOWLEDGEMENTS

We extend our sincere gratitude to Dr. David Oliver, Jade Muileboom, Brynn McMillan, and the teaching team for their guidance and support throughout our project. Their expertise significantly contributed to the ongoing success of our endeavors. We would also like to express our gratitude to Goh et al. for providing the pENS plasmid and the Department of Botany for providing the *A. thaliana* seeds. Additionally, we express our appreciation to the Department of Microbiology and Immunology at the University of British Columbia for their generous funding and provision of laboratory facilities, which were instrumental in facilitating our research. Lastly, we would like to thank each other for our hard work in the lab and mutual support. We would also like to thank two anonymous reviewers for constructive feedback on this manuscript.

CONTRIBUTIONS

As a collaborative effort, all team members (AW, DL, KZ, and TW) contributed equally to all sections of the draft manuscript, and lab work and provided valuable feedback, which was instrumental in shaping the project.

REFERENCES

1. **Han W, Zhao R, Liu W, Wang Y, Zhang S, Zhao K, Nie J.** 2023. Environmental contamination characteristics of heavy metals from abandoned lead–zinc mine tailings in China. *Front Earth Sci* **11:**1082714.
2. **Da Silva-Rêgo LL, De Almeida LA, Gasparotto J.** 2022. Toxicological effects of mining hazard elements. Energy Geoscience **3**:255–262.
3. **Kaur H, Garg N.** 2021. Zinc toxicity in plants: a review. *Planta* **253:**129.
4. **Azubuike CC, Chikere CB, Okpokwasili GC.** 2016. Bioremediation techniques–classification based on site of application: principles, advantages, limitations and prospects. *World J Microbiol Biotechnol* **32:**180.
5. **Rajendran S, Priya TAK, Khoo KS, Hoang TKA, Ng H-S, Munawaroh HSH, Karaman C, Orooji Y, Show PL.** 2022. A critical review on various remediation approaches for heavy metal contaminants removal from contaminated soils. *Chemosphere* **287:**132369.
6. **Lu C-W, Ho H-C, Yao C-L, Tseng T-Y, Kao C-M, Chen S-C.** 2023. Bioremediation potential of cadmium by recombinant *Escherichia coli* surface expressing metallothionein MTT5 from *Tetrahymena thermophila*. *Chemosphere* **310:**136850.
7. **Díaz S, Amaro F, Rico D, Campos V, Benítez L, Martín-González A, Hamilton EP, Orias E, Gutiérrez JC.** 2007. *Tetrahymena Metallothioneins* Fall into Two Discrete Subfamilies. *PLoS ONE* **2:**e291.
8. **Espart A, Marín M, Gil-Moreno S, Palacios Ò, Amaro F, Martín-González A, Gutiérrez JC, Capdevila M, Atrian S.** 2015. Hints for Metal-Preference Protein Sequence Determinants: Different Metal Binding Features of the Five *Tetrahymena thermophila* Metallothioneins. *Int J Biol Sci* **11:**456–471.
9. **Wang J, Moeen-ud-din M, Yang S.** 2021. Dose-dependent responses of *Arabidopsis thaliana* to zinc are mediated by auxin homeostasis and transport. *Environmental and Experimental Botany* **189:**104554.
10. **Nicchi S, Giuliani M, Giusti F, Pancotto L, Maione D, Delany I, Galeotti CL, Brettoni C.** 2021. Decorating the surface of *Escherichia coli* with bacterial lipoproteins: a comparative analysis of different display systems. *Microb Cell Fact* **20**:33.
11. **Fan E, Chauhan N, Udatha DBRKG, Leo JC, Linke D.** 2016. Type V Secretion Systems in Bacteria. *Microbiol Spectr* **4:**4.1.10.
12. **Rutherford N, Mourez M.** 2006. Surface display of proteins by Gram-negative bacterial autotransporters. *Microb Cell Fact* **5:**22.
13. **Sun F, Pang X, Xie T, Zhai Y, Wang G, Sun F.** 2015. BrkAutoDisplay: functional display of multiple exogenous proteins on the surface of *Escherichia coli* by using BrkA autotransporter. *Microb Cell Fact* **14:**129.

14. **Santovito G, Formigari A, Boldrin F, Piccinni E.** 2007. Molecular and functional evolution of *Tetrahymena* metallothioneins: New insights into the gene family of *Tetrahymena thermophila*. *Comparative Biochemistry and Physiology Part C: Toxicology & Pharmacology* **144:**391–397.
15. **Chen X, Zaro JL, Shen W-C.** 2013. Fusion protein linkers: Property, design and functionality. *Advanced Drug Delivery Reviews* **65:**1357–1369.
16. **Goh J, Tan D, Yu C, Zaidi A.** 2024. Engineering an OmpT cleavage site in the BrkA passenger domain to explore the role of the conserved autochaperone region. UJEMI+ [Preprint].
17. **Oliver DC, Huang G, Fernandez RC.** 2003. Identification of Secretion Determinants of the *Bordetella pertussis* BrkA Autotransporter. *J Bacteriol* **185:**489–495
18. **Jumper J, Evans R, Pritzel A, Green T, Figurnov M, Ronneberger O, Tunyasuvunakool K, Bates R, Žídek A, Potapenko A, Bridgland A, Meyer C, Kohl SAA, Ballard AJ, Cowie A, Romera-Paredes B, Nikolov S, Jain R, Adler J, Back T, Petersen S, Reiman D, Clancy E, Zielinski M, Steinegger M, Pacholska M, Berghammer T, Bodenstein S, Silver D, Vinyals O, Senior AW, Kavukcuoglu K, Kohli P, Hassabis D.** 2021. Highly accurate protein structure prediction with AlphaFold. *Nature* **596:**583–589.
19. **Blanch-Asensio M, Dey S, Sankaran S.** 2023. *In vitro* assembly of plasmid DNA for direct cloning in *Lactiplantibacillus plantarum* WCSF1. *PLoS ONE* **18**:e0281625.
20. **Kato Y.** 2020. Extremely Low Leakage Expression Systems Using Dual Transcriptional-Translational Control for Toxic Protein Production. *IJMS* **21:**705.
21. **Jose J, Krämer J, Klauser T, Pohlner J, Meyer TF.** 1996. Absence of periplasmic DsbA oxidoreductase facilitates export of cysteine-containing passenger proteins to the *Escherichia coli* cell surface via the Igaβ autotransporter pathway. *Gene* **178:**107–110.
22. **Klauser T, Pohlner J, Meyer TF.** 1992. Selective extracellular release of cholera toxin B subunit by *Escherichia coli:* dissection of *Neisseria* Iga beta-mediated outer membrane transport. *The EMBO Journal* **11**:2327–2335.
23. **Yang P-C, Mahmood** T. 2012. Western blot: Technique, theory, and trouble shooting. *North Am J Med Sci* **4:**429.
24. **Chen G, Strevett KA.** 2003. Impact of carbon and nitrogen conditions on *E. coli* surface thermodynamics. *Colloids and Surfaces B: Biointerfaces* **28:**135–146.
25. **Leifert C, Waites WM.** 1992. Bacterial growth in plant tissue culture media. *Journal of Applied Bacteriology* **72:**460–466.
26. **De Francisco P, Melgar LM, Díaz S, Martín-González A, Gutiérrez JC.** 2016. The Tetrahymena metallothionein gene family: twenty-one new cDNAs, molecular characterization, phylogenetic study and comparative analysis of the gene expression under different abiotic stressors. BMC Genomics **17**:346.
27. **Rebello S, Nathan VK, Sindhu R, Binod P, Awasthi MK, Pandey A.** 2021. Bioengineered microbes for soil health restoration: present status and future. Bioengineered **12**:12839–12853.